ACS OMEGA

http://pubs.acs.org/journal/acsodf

Article

Competitive Adsorption of Caffeine and Diclofenac Sodium onto Biochars Derived from Fique Bagasse: An Immersion Calorimetry Study

Yaned Milena Correa-Navarro, Juan Carlos Moreno-Piraján,* and Liliana Giraldo

Cite This: *ACS Omega* 2023, 8, 1967−1978

Read Online

ACCESS | Metrics & More | Article Recommendations | Supporting Information

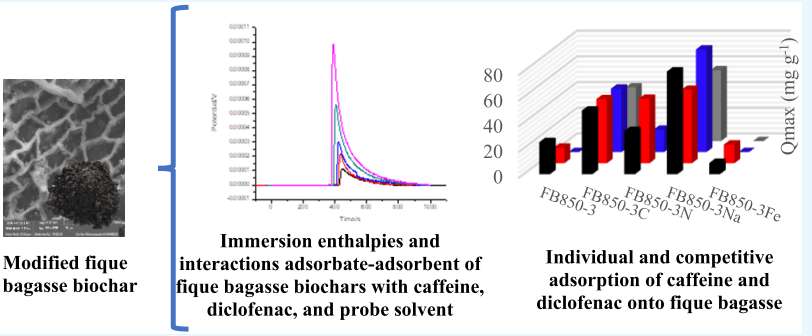

ABSTRACT: Pharmaceuticals, including caffeine (CFN) and diclofenac sodium (DCF), are a group of emerging pollutants which have the capacity to prompt harmful effects in flora and fauna, even at relatively low concentrations. Additionally, CFN has been determined as one of the most ubiquitous active compounds in the natural environment, whereas DCF is a widely used nonsteroidal anti-inflammatory drug that has been detected in environmental sources around the world. Conversely, the fique is a plant of the Agavaceae family and of the Fucraea genus.Two native species are cultivated in Colombia, *Furcraea cabuya* and *Furcrae macrophylla*, in order to extract their fiber, but in this process a lot of waste is produced. In this study, with the fique residues, thermochemical treatments were carried out and 5 biochar samples were obtained, which were calorimetrically characterized and used to investigate their behavior in competitive adsorption of DCF and CFN. The results of the calorimetric studies show that the biochar prepared from fique bagasse have different porous and chemical characteristics, which is related to the different treatments that were used at the time of their preparation. In addition, it was established that the results of the adsorbate−adsorbent interactions determined by calorimetry allow correlation of the adsorption processes of the molecules under study (CFN and DCF). The results show that the NaOH fique biochar (FB850-3Na) presents the highest adsorption capacity in both simple and competitive tests.

1. INTRODUCTION

When the word pollutant is mentioned, it is associated with the different industrial-type processes that have led to environmental pollution through different molecules. That is why those who research in this area have proposed to solve this problem from different areas. One of these widely used processes is adsorption, because it allows solids to be prepared with a high specificity for each of the molecules to be removed from an ecosystem and also because waste raw materials are commonly used, which makes it very inexpensive and scalable to the communities of each country, especially those in the process of development. In the case of fique waste, its technological, environmental, and biological importance in this type of process cannot be doubted. In addition, its practical applications in industry and environmental protection are of the highest importance, as for example, in the adsorption process, which usually becomes a first step in certain catalytic processes and mixing methods. Furthermore, for problems such as the purification of water, air, and soil, adsorption processes are also required.[1] On the other hand, in environmental research studies it is common to analyze pollutants simultaneously, and many of these are removed by adsorption. In the scientific literature it has been reported that in some cases these pollutants compete for active sites of the adsorbent.[2] For this reason, in pollutant adsorption studies it is important to determine the adsorption capacity of the adsorbent in a competitive way in order to get closer to what a real system can be.

Received: August 1, 2022
Accepted: November 1, 2022
Published: December 30, 2022

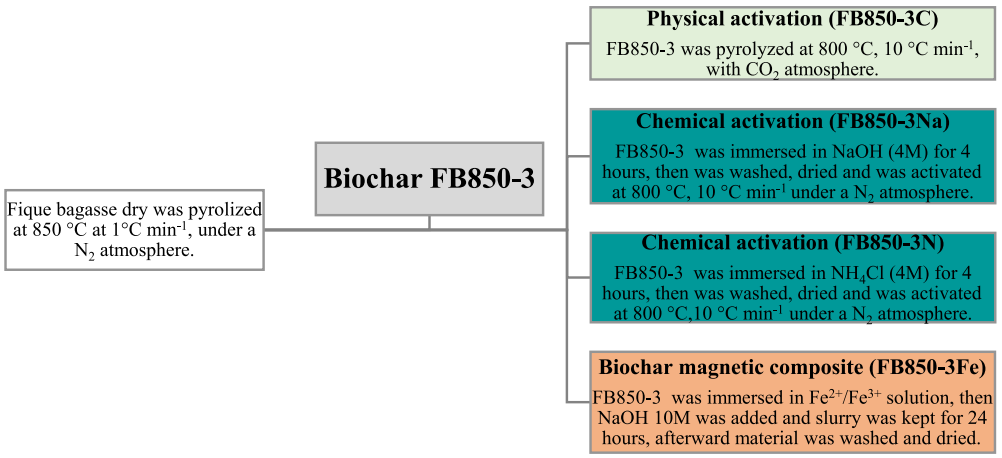

Figure 1. Schematic to obtain fique bagasse biochar modified.

Recently, within many pollutants found in aquifers, a large number of emerging-type compounds have been detected, which not only are very harmful for the ecosystem but ultimately affect human health. Thus, it is interesting to propose solutions to face this problem. Among these substances we can mention caffeine and diclofenac sodium. Caffeine is an alkaloid used as a stimulant of the nervous and respiratory systems, and this substance with active behavior is the most consumed worldwide with an average of 70−76 mg per person per day. This, in addition to its high solubility (21.6 g L^{-1}) and its low octanol−water partition coefficient (log K_{ow} = 0.16), is one of the reasons why caffeine is frequently found in surface waters and wastewater.[3] Additionally, diclofenac sodium is a nonsteroidal anti-inflammatory drug (NSAID) widely used for the treatment of pain and inflammation in both humans and animals. The global consumption of this drug was estimated at around 1,443 ± 58 tons per year,[4] and it is among the 10 most commonly detected compounds in aquatic environments.[5]

Biochar as a porous solid has been used in numerous applications, such as soil remediation, waste treatment, greenhouse gas reduction, energy production, and pollutant adsorption.[6,7] The term biochar refers to a solid product that remains after a biomass is subjected to a heat treatment that can vary, but that usually ranges between 300 and 700 °C in the absence of oxygen (called atmospheric inert), which is achieved by injecting nitrogen. This process is known as pyrolysis. In contrast to the raw material of the original biomass that contains mainly cellulose, hemicellulose, and lignin, biochar falls into the spectrum of materials usually called "charcoal" or "black carbon".[8] Many agro-industrial biomass residues are rich in carbon, which makes them an attractive alternative to produce carbonaceous materials. In fact, several researchers have been studying the preparation of biochar from this type of waste, such as the husk of coconut, bagasse from sugar cane, residues from the African oil palm coat, rice husk, palm kernel husk, and pine wood chips, among others.[9,10]

In Colombia, fique bagasse is an agro-industrial waste derived from the fique fiber extraction process that generates a byproduct that is almost 25% by weight with respect to the fique leaf. Unfortunately, it is normal for this waste to be left to decompose in the crop or discarded in aquifers, which generates the problem of environmental contamination.[11] Therefore, it is important to look for alternatives for the use of this biomass and to be able to socialize these alternatives with the communities.

On the other hand, after the preparation of a biochar and before exploring its possible applications, the chemical and morphological characterization of these carbonaceous solids is important. Study of their different properties such as surface area, porosity, pH, surface charge, and mineral content, among others, is responsible for the technological uses of these materials and finally for their possible application in environmental remediation and their possible scaling.[12] Additionally, the quantification of the adsorbent−adsorbate interactions is of utmost importance because the energetic part that is involved in this type of interactions is established in this way, and these properties can be determined by means of different experimental techniques such as isotherm experiments of adhesion at different temperatures and application of the Clausius−Clapeyron equation. However, immersion calorimetry is a technique that is not widely used, not only because of the cost of the equipment but especially because it requires a lot of care from an experimental point of view, yet it is very precise because it is a direct measure of adsorbate−adsorbent interactions.[13,14]

Nevertheless, the study of each adsorbent as well as adsorbate−adsorbent interactions has become a new challenge when researching new adsorbents and their application in the retention of certain contaminants. Using calorimetry to analyze this process is very interesting. There is still a lack of information in the scientific literature that clearly establishes the type of interactions between adsorbate−adsorbent from thermodynamics, using a material as novel as fique and correlating it with simple and competitive adsorption isotherms in emerging-type pollutant molecules. That is why this research was approached, with the aim of studying the type of interactions that occur between five biochar materials prepared from fique waste in different probe molecules, using immersion calorimetry. Finally, the competitive adsorption capacity of caffeine and diclofenac sodium in the five-fique bagasse biochar was determined.

2. MATERIALS AND METHODS

2.1. Biochar Preparation. The procedure followed to prepare and modify the different biochars in this research is detailed in a publication by Correa et al.[15] A summary of this procedure follows: Initially, a quantity of fique bagasse (FB) is placed in a cell made of steel. The pyrolysis process was then

https://doi.org/10.1021/acsomega.2c04872
ACS Omega 2023, 8, 1967−1978

started at a temperature of 850 °C with a heating rate of 1 °C min^{-1} under a nitrogen atmosphere for 3 h. The material in this study was labeled as FB850-3. The values of the variable's temperature, heating speed, and holding time were established in previous tests.

Then four modifications were made as follows: In the first, CO_2 was used as the activation gas. For this method, the sample FB850-3 was heated between 25 and 800 °C at 10 °C min^{-1}, with CO_2 at a flow rate of 100 mL min^{-1} for 2 h. This biochar was labeled FB850-3C. The second and third methods of modification were chemical activations. In both procedures, the FB850-3 sample was immersed in NaOH (4M) or NH_4Cl (4 M) with a mass ratio of 1:10 at room temperature for 4 h. After this, the biochar was dried. Finally, the carbonaceous material was charred at 25−800 °C for 2 h under nitrogen flow. These biochars were labeled FB850-3Na and FB850-3N, respectively. The last modification method was carried out with magnetite, which included coprecipitation and coating of FB850-3 with Fe^{3+}/ Fe^{2+}. This biochar was labeled FB850-3Fe (Figure 1). It is important emphasized that after pyrolysis all biochars were washed with purified water until the pH of the filtrates was constant. The washed activated biochars were dried in an oven at 110 °C and stored for analysis.

2.2. Immersion Calorimetry Measurements. In order to acquire information that allows an adequate understanding of the interactions between the adsorbate−adsorbent, various analytical techniques have been used. However, immersion calorimetry is a little explored technique that allows characterization of the adsorption−adsorbent systems. Of the different types of calorimetry, the one that is adequate to address this type of study is immersion calorimetry. By means of immersion calorimetry it is possible to measure immersion enthalpy (ΔH_{imm}), which is defined as the change in enthalpy, at constant temperature and pressure, that occurs when a solid is immersed in a liquid in which it does not dissolve or react.[16]

2.3. Description of the Immersion Calorimeter. The measurements reported in this research were performed in a "homemade" immersion calorimeter developed in our laboratory.[17,18] It should be considered that to achieve correct measurements and reproducible experiments in immersion calorimetry the researcher must take into account that different energy sources are involved in each experimental measurement. Therefore, the heat that is recorded in an immersion experiment is the sum of different contributions as shown in eq 1[19]

$$Q_{exp} = \Delta_{imm}U + W_b + \int_0^{V-v} PdV + \frac{\Delta_{liq}h}{RT}[(P - P^o)V + P^o v] \quad (1)$$

where $\delta_{imm}u$ = immersion energy; W_b= breakup vial; $\int_0^{V-v} PdV$ = vapor compression in the bulb; $\frac{\Delta_{liq}h}{RT}[(P - P^o)V + P^o v]$ = liquefaction of the liquid in the bulb (v) and liquid vaporization outside the bulb (V).

If experiments are carried out with glass vials of different sizes and performing a statistical analysis, each of these terms can be correctly evaluated, and in this way the measurements taken by immersion calorimetry will be correct.[18] It is important to highlight this aspect because researchers who are not close to calorimetry omit it, generating results that have high uncertainties and in many cases are not reproducible and, therefore, prevent the possibility of examining the true scope of this methodology. The equipment used in this work is described in the Supporting Information.

2.4. Experimental Immersion Calorimetry. An experimental series of immersion calorimetries was carried out by placing 0.1 ± 0.0001 g of the biochars prepared in this study inside the glass bulb. The sample is desorbed at a temperature of 100 °C and a vacuum of 10^{-5} mbar for 3 h. Next, the glass bulb is sealed, and it is placed inside the calorimeter in the bulb holder; simultaneously, 10 mL of the respective immersion liquid to be examined is placed in the calorimetric cell. It is necessary to wait for the electrical signal to stabilize until the baseline has a signal no greater than ±0.5 μV. When this happens, the calorimetric system is ready under thermodynamic conditions to proceed to break the vial and to record the thermal effect until the signal returns to the baseline. Next, the electrical type of calibration is carried out, which must be performed with each experimental measurement. Finally, the corrections corresponding to the breaking of the glass bulb and the evaporation of the liquid within the same bulb are carried out by repeating the experiments with empty bulbs.

Figure 2 shows a typical thermogram where the first peak that corresponds to the adsorbate−adsorbent interaction and

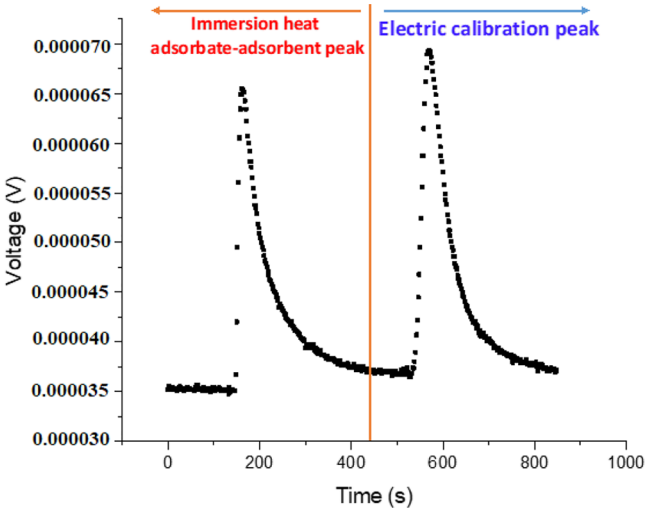

Figure 2. Calorimetric curve of FB850-3N biochar into water (the first peak is the immersion peak while the second is the calibration peak).

the second corresponds to the electrical calibration. Using eqs 2−5 allows to obtain the respective enthalpies of adsorption of each experimental determination[20,21]

$$\Delta H_{imm} = \frac{Q_{inm}(J)}{\text{biochar mass}(g)} \quad (2)$$

$$Q_{imm=}K_{cal}\cdot\text{area under curve(calibration peak)} \quad (3)$$

$$K_{cal} = \frac{W_{el}}{\text{area under curve(calibration peak)}} \quad (4)$$

$$W_{el} = \text{voltage (V)}\cdot\text{current (A)}\cdot\text{time (s)} \quad (5)$$

where ΔH_{imm} is the immersion enthalpy, Q_{imm} is the heat of immersion, K_{cal} is the constant of the calorimeter, and W_{el} is the electrical work from electrical calibration.

The enthalpies of interaction between caffeine (CFN) and diclofenac sodium (DCF) (ΔH_{int} CFN or DCF) were also

https://doi.org/10.1021/acsomega.2c04872
ACS Omega 2023, 8, 1967−1978

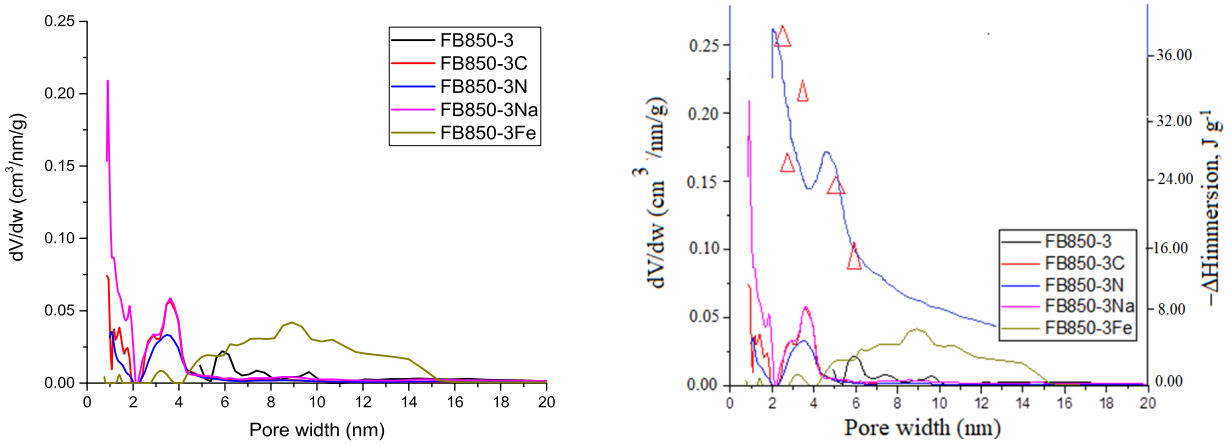

Figure 3. Pore-size distribution for fique bagasse biochars. (a) PSD derived from N_2 at −196.15 °C isotherms. (b) Comparison of the immersion enthalpies with the probe molecules with the sample FB850-3Na with the PSDs from isotherms of N_2 −196.15 °C.

determined using Hess's law; for this determination it was assumed that the solutions are at infinite dilution. Therefore, to calculate the enthalpy of the interaction in this work, eq 6 was used

$$\Delta H_{int} = \Delta H_{imm(CFN\ or\ DCF)} - \Delta H_{imm(H2O)} \quad (6)$$

where $\Delta H_{imm(CFN\ or\ DCF)}$ is the immersion enthalpy into CFN or DCF solutions at 50.0 mg L^{-1} and $\Delta H_{imm(H2O)}$ is the immersion enthalpy in water.

In this way, in this research, five experimental determinations were made between the liquid and each FB sample, and average values of the immersion enthalpy were considered. For the adsorbents prepared in this work, FB850-3, FB850-3C, FB850-3N, FB850-3Na, and FB850-3Fe, the following liquids with different molecular diameter: water 0.28 nm, methanol 0.43 nm, *t*-butanol 0.60 nm, α-pinene 0.70 nm, benzene 0.37 nm, and dichloromethane 0.33 nm.[19,22,23] With these molecules the immersion enthalpies were determined. To make the calorimetric blanks additional experiments were carried out using double-distilled and deionized water. The immersion enthalpies were also determined for solutions of diclofenac sodium and caffeine.

2.5. Competitive Adsorption Procedure. To start with, stock solutions of caffeine (CFN) and diclofenac sodium (DCF) were prepared in ultrapure water. Afterward, different volumes of each compound solution were taken to prepare mixtures of these two substances at different concentrations (Table S1). Thereafter, 5.0 mL of each mixture was placed in a glass vial and put in contact with 20.0 mg of each of the biochar evaluated; after that, the vessels were placed in an orbital shaker and shaken for 48 h at 20.0 °C. Finally, a sample of each solution was taken, filtered, and analyzed by high performance liquid chromatography (HPLC) to obtain the amount of caffeine and diclofenac adsorbed at equilibrium Q_e (mg g^{-1}) using eq 7. Consequently, the data obtained were used with the isotherm mathematical models shown in Table S2

$$Q_e = \frac{V(C_o - C_e)}{m} \quad (7)$$

where C_o and C_e correspond to the initial and equilibrium concentrations of CFN or DCF, respectively (mg L^{-1}), V is the volume of solution (L) and m is the mass of the biochar used in each determination (g).

2.6. Analytical Method. For qualification and quantification by HPLC, a Thermo Scientific UltiMate 3000 UHPLC instrument with a diode array detector (DAD) coupled to an ion trap analyzer mass spectrometer using an electrospray ionization (ESI) source operated in positive mode was used. In addition, the instrument was controlled with Xcalibur 3.0 software (Thermo Scientific). Before analysis, all aqueous solutions were filtered through 0.22 μm PTFE membranes. Chromatographic analyses were performed on a reversed-phase Prontosil C18 column (4.0 × 125 mm, 5 μm, 100 Å), and the column temperature was kept at 40 °C. Acetonitrile and water (containing 0.1% phosphoric acid) (6:4, v/v) were used as the mobile phase at a flow rate of 0.5 mL min^{-1}. 10.0 μL of sample was injected using an autosampling device; additionally, caffeine was detected at 274 nm, while diclofenac was found at 273 nm and DAD was used in a range of 190−290 nm. Finally, confirmation of compounds was possible by employing a mass spectrometric (MS) detector using the following parameters in the ESI source: a spray voltage of 5.5 kV, a capillary temperature of 330 °C, sheath gas flow 9 arbitrary units, and auxiliary gas flow 2 arbitrary units. The ion trap was configured to operate in full scan (m/z mass range 65−1200) and MS/MS mode dependent with collision energy at 30% to metabolites, with an isolation width of 3 m/z.

The HPLC assays required preparation and subsequent evaluation of caffeine and diclofenac calibration curves. For this purpose, standard solutions of 1000 mg L^{-1} of both analytes were prepared in ultrapure water, and from these, all of the standards of CFN and DCF needed for the different analyses were obtained. In all cases, spectra of the solutions were recorded over time in order to verify the stability of the molecules under study. All samples were evaluated in triplicate.

3. RESULTS AND DISCUSSION

3.1. Calorimetric Experiments. The apparent surface area and the pore size distribution (PSD) of the fique bagasse biochars (FBB) worked in this study were previously calculated using the Brunauer−Emmett−Teller (BET) models and the quenched solid density functional theory (QSDFT) model using the isotherm data from N_2 at −196.15 °C and using the IQ2 sortometer software (isotherms are not shown here; only the PSDs using the QSDFT model, for comparison purposes). Figure 3 shows the results obtained for the PSD for the FBB using the results of the N_2 isotherms at −196.15 °C.

https://doi.org/10.1021/acsomega.2c04872
ACS Omega 2023, 8, 1967−1978

The results shown in Figure 3a,b are very interesting from the perspective of the analysis of the PSD obtained from the isotherms with N_2 at −196.15 °C and comparing the enthalpies obtained with the probe molecules of different molecular diameters. Figure 3a shows that there is a broad spectrum and significant differences between the PSDs corresponding to the biochars prepared from fique bagasse. It can be seen that the FB850-3Na sample was the biochar that developed the highest microporosity and later presented a peak of average size in the range 2.0−4.0 nm, which can be attributed to the beginning of the development of an insipient mesoporosity. When the PSD of the bicochar FB850-3Fe was analyzed, this sample was the one that developed the least porosity and was found within a low mesoporsity to later develop larger porosities of the macropore type. In the case of FB850-3Na, a pore width was detected in the micropore range centered at 0.8 nm with the distribution extending approximately 1.0 nm on either side of it and a shoulder extending to 4.0 nm. The biochars FB850-3C and FB850-3N indicate the presence of some micropores, according to PSD Figure 3a, with peaks of less intensity. In contrast, the other biochars do not show the development of micropores.

To establish a PSD by immersion calorimetry and to compare the results with those obtained by the QSDFT model, in this work different probe molecules with different kinetic diameters ranging from 0.33 to 0.70 nm were used.

To illustrate how immersion enthalpies in different probe molecules can be interpreted and analyzed, enthalpy values for sample FB850-3Na were plotted in Figure 3b. With the data, an approximate behavior has been traced within the range of the diameter of the analyzed molecules, observing that there is a similar trend between the PSDs evaluated from the N_2 isotherms at −196.15 °C and what we could call the "calorimetric PSD". These results obtained from the immersion calorimetry show that with this technique it is possible to get closer to establishing a PSD of the samples as has been done in this research.

Figure 4 presents the immersion enthalpy values obtained for each FBB sample in each of the probe molecules of different molecular size. The lines that are drawn only represent a trend and not the actual behavior. In general, the results shown in Figure 4 show that the enthalpy values decrease as a function of the size of the probe molecule used. If, for example, the values of immersion enthalpy in benzene (C_6H_6) and dichloromethane (CH_2Cl_2) are observed then solvents of smaller molecular size are used, 0.37 and 0.33 nm, respectively, corresponding to the highest ones, while with α-pinene, which is the molecule with the largest molecular size, 0.70 nm, the ΔH_{imm} values are lower. This is associated with how each of the molecules can enter the pores developed by the treatment to the fique bagasse. The smallest molecules manage to enter more "easily", generating these interactions with the graphitic plates and as a result the highest enthalpic values.

When the results of Figure 4 are examined in detail; the ΔH_{imm} values show in a general way that they are heterogeneous and are undoubtedly associated with the same property of the surfaces of solids prepared from fique bagasse.

The samples FB850-3, FB850-3C, and FB850-3Fe did not present great differences between the values of ΔH_{imm} with the molecules CH_2Cl_2 and C_6H_6, while the FB850-3N sample had the highest ΔH_{imm} value when immersed in C_6H_6 and the FB850-3Na sample had the highest ΔH_{imm} value with CH_2Cl_2.

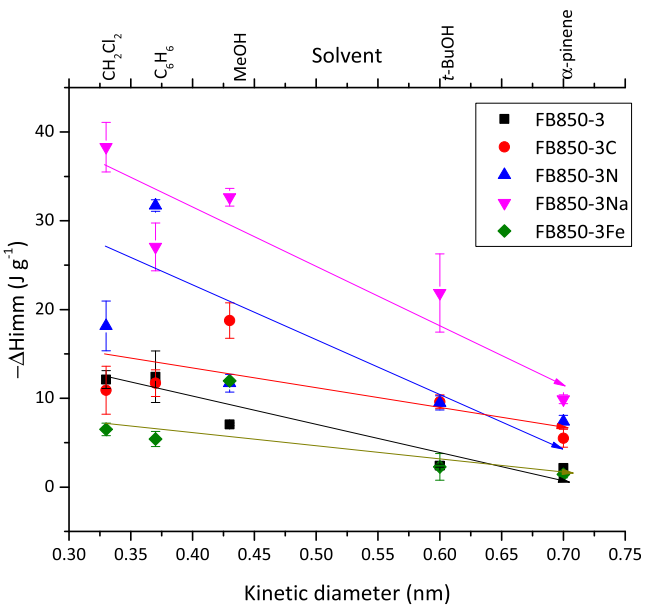

Figure 4. Relationship between the immersion enthalpy of fique bagasse biochars with solvents of different kinetic diameters evaluated (the lines correspond to the linear trend of each data series).

This suggests that the FB850-3N sample presented a pore distribution such that it allowed the benzene molecule to enter to its porous structure, giving the highest value of enthalpy; this is apparent when compared to the PSD evaluated by means of the QSDFT models where slit-shaped pores are assumed for its calculation. Thus, it can be argued that the benzene molecule can enter this type of pore if benzene is modeled as a reasonably flat molecule.

Figure 4 shows that there was a negative trend between the kinetic diameter of the solvents and the fique bagasse biochars evaluated. In other words, with benzene (C_6H_6) and dichloromethane (CH_2Cl_2), which were the lowest molecular size solvents used at0.37 and 0.33 nm, respectively, values of immersion enthalpies were higher, while with α-pinene, which was the molecule with the largest molecular size of 0.70 nm values of ΔH_{imm} were lower. In turn, values of ΔH_{imm} evidenced heterogeneity on the surface of the FBB studied; in the case of FB850-3, FB850-3C, and FB850-3Fe it did not show wide differences between the values of ΔH_{imm} with CH_2Cl_2 and C_6H_6, while FB850-N had the highest ΔH_{imm} with C_6H_6 and FB850-3Na had a higher ΔH_{imm} value with CH_2Cl_2.

This suggested that FB850-3N exhibited a suitable pore distribution for benzene adsorption as well as slit-shaped pores that allowed the entry of a flat molecule such as benzene; meanwhile, FB850-Na is likely to have pores of a cylindrical type, which restricted the entry of benzene. This is congruent with the enthalpy values obtained. Furthermore, when considering the surface functional groups present in the FBB850-3Na sample, they favor dipole−dipole interactions (polarity of benzene and dichloromethane: 0.00 and 1.55 D), which justifies the increase in ΔH_{imm} of FB850-Na in CH_2Cl_2. This statement reflects that this sample showed the same behavior with other evaluated polar solvents: MeOH and *t*-BuOH, (1.70 and 1.66 D).

Additionally, the immersion enthalpy values determined for CH_2Cl_2 (0.33 nm), which is a molecule of similar size to N_2 (0.36 nm), allowed us to establish that the surface area increased as follows: FB850-3Na > FB850-3N > FB850-3 ≥

https://doi.org/10.1021/acsomega.2c04872
ACS Omega 2023, 8, 1967−1978

Table 1. Immersion Enthalpies of Fique Bagasse Biochars in Benzene, Water and Caffeine and Diclofenac Solutions at 50 mg L^{-1}[a]

	$-\Delta H_{imm}$ (J g^{-1})				
Sample	C_6H_6	H_2O	CFN	DCF	$f_h = \frac{\Delta H_{imm} C_6H_6}{\Delta H_{imm} H_2O}$
FB850-3	12.4 ± 1.4	20.1 ± 0.4	18.1 ± 1.2	18.9 ± 1.8	0.619
FB850-3C	11.7 ± 1.5	5.8 ± 0.4	12.9 ± 1.2	10.7 ± 1.4	2.02
FB850-3N	31.7 ± 0.6	22.3 ± 1.8	22.0 ± 1.8	16.6 ± 1.6	1.42
FB850-3Na	27.1 ± 1.7	18.9 ± 0.5	4.4 ± 0.4	12.4 ± 1.9	1.43
FB880-3Fe	5.4 ± 0.8	21.2 ± 1.0	10.2 ± 1.5	16.5 ± 0.9	0.255

[a]ΔH_{imm} = immersion enthalpy; f_h = hydrophobic factor.

FB850-3C > FB850-3Fe (this approximation can be concluded assuming that there are no effects caused by the filling of micropores). Meanwhile, the values that were calculated using the N_2 adsorption isotherms show an increase in the apparent surface area as follows: 442, 302, 212, 105, and 90 m^2 g^{-1}, respectively. These two results support what was explained previously; with these two techniques it is possible to infer the apparent surface, although there is variability between the data determined by ΔH_{imm} originated by several factors.[24,25] In addition, these results showed that the NaOH-treated biochar increased the volume and broadened the pore size distribution, which was evidenced by the strong increase in the immersion enthalpy determined by changing the molecular size of the solvents used, in comparison with that shown by the other biochars, in which the increase in immersion enthalpy was less pronounced, and this was attributed to a small change in the width of the pores. These results were correlated with the pore distribution obtained by N_2 adsorption in which FB850-3Na was the biochar that presented the highest proportion of microporosity.

As it has been shown, the immersion calorimetry enables an adequate correlation between the PSD calculated from the N_2 isotherms at −196.15 °C using the modeling method based on the QSDFT and the results when the adsorbent is immersed in molecules with different molecular diameter. This shows that it is possible to approach the adsorption capacities study of different compounds that are being studied in this work from the immersion calorimetry and correlate the enthalpies generated by the adsorbate−adsorbent interaction with the structure of the adsorbent and the molecule; immersion calorimetry is considered to be one of the most reliable techniques for the quantification of energies in this type of interaction.[26] The values of the immersion enthalpies (ΔH_{imm}) of the bagasse biochars in benzene, water, CFN, and DCF in this study are presented in Table 1.

The immersion enthalpy values (Table 1) that showed the most significant differences when the immersion tests were carried out in solvents of different polarity such as water and benzene (1.855 and 0.111 D, respectively) were the biochars FB850-3N and FB850-3Na, which presented the highest enthalpy values of ΔH_{imm} in benzene. Besides the information presented in the paragraphs above related to the fact that these materials had a distribution of pores that allowed the entry of the benzene molecule into its porous structure, this result can also be associated with the data obtained from the atomic relation H/C in which these biochars have a high aromaticity.[15] These results suggest that the samples FB850-3N and FB850-3Na have regions with high electron densities in the graphene layers, thus generating donor−acceptor interactions with delocalized π electrons that show that the samples of FBB and benzene were the most effective and had stronger interactions resulting in higher enthalpic values. With the samples FB850-3, FB850-3C, and FB850-Fe these electronic interactions were of lower value, and therefore, their enthalpies were too. Consequently, the results obtained by immersion calorimetry allow the analysis of the interactions that occur between the samples prepared from fique bagasse, establishing that the chemical interactions are more effective between FB850-3Na and FB850-3N with nonpolar molecules than with polar ones. Regarding the immersion enthalpy values that were obtained with the water molecule, the values in general are very similar except for the sample FB850-3C. This result leads into the inference that the oxygenated surface functional groups available in the FBB are capable of carrying out dipole−dipole interactions with hydrogen bonds and, in the case of starting from this magnetic material, between ion−dipole interactions ($Fe^{+}_{x}{}^{-}OH$) with water.[14]

In order to analyze the behavior between the hydrophobic factor and the immersion enthalpies in DCF and CFN, the results were plotted and are shown in Figure 5. There it can be

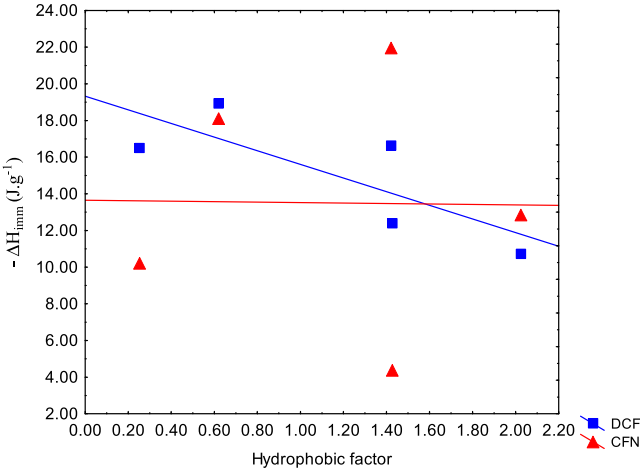

Figure 5. Correlation between ΔH_{imm} in DCF and CFN in FBB samples prepared.

observed that for the DCF molecule there is a reasonably linear correlation while for the CFN molecule the values are more dispersed, and a correlation cannot really be established for this molecule. With the FB850-3, FB850-3N, and FB850-3Fe biochars, the highest enthalpy values were obtained when immersed in CFN and DCF solutions. These results can be interpreted considering that the biochars prepared from the fique bagasse present interactions of the Van der Walls type with the functional groups of the surface with the DCF and

https://doi.org/10.1021/acsomega.2c04872
ACS Omega 2023, 8, 1967−1978

CFN molecules, as well as scattering interactions between the π electrons of the layers of graphene that allowed the enthalpy magnitude to behave in this way.[16,27]

On the other hand, Figure 6 shows the results obtained for each of the biochar samples based on their adsorption capacity

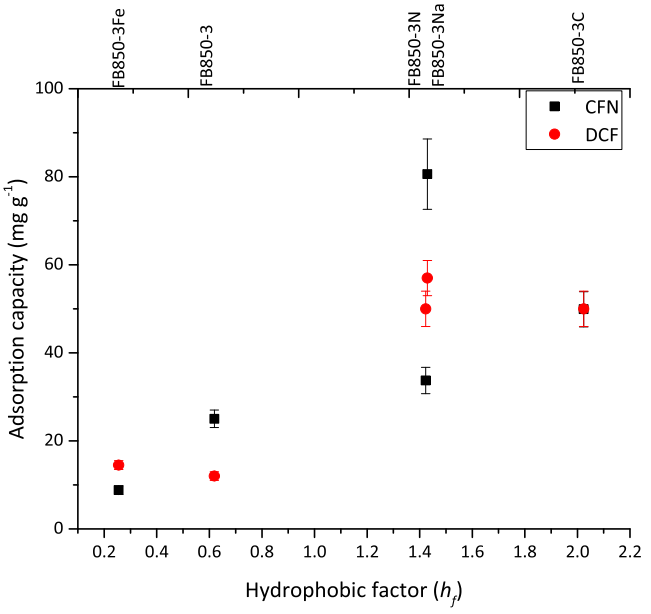

Figure 6. Relationship between the hydrophobic factor and the maximum adsorption capacity of the fique bagasse biochars evaluated.

for the DCF and CFN molecules and the hydrophobic factor. These results show that for DCF the adsorption capacity increases as the hydrophobic factor increases, showing that a direct relationship between the hydrophobicity factor was evaluated. Here again, a clearly linear correlation can be seen. For the CFN molecule, its adsorption capacity also increases as a function of the hydrophobic factor, but the results are more dispersed. According to Figure 6, the highest adsorption capacities are reached for samples F850-3N and F850-3Na. These results agree with what was previously discussed with those obtained with immersion calorimetry since it is observed that the adsorption capacity of the biochars prepared in this research is directly related to the surface chemistry and the porosity of the prepared adsorbent.

Figure 7 shows in the form of a histogram the enthalpies of the interactions (ΔH_{int}) between the different FBB samples and the caffeine molecules, diclofenac, in water. It can be seen that the enthalpies corresponding to the interactions with these molecules were lower than ΔH_{int} of these same biochars when they were placed in contact with water, except for the sample FB850-3C.

Thanks to this, it is possible to infer that the values of the immersion enthalpies measured (by immersion calorimetry) are associated with the H_2O−adsorbent interactions; they decreased with the presence of CFN and DCF. These results suggest that to overcome the attractive forces of the adsorbent H_2O it was necessary to obtain energy from the environment to displace the water from the surface of the FBB and achieve the desolvation of CFN and DCF. On the other hand, for the FB850-3C sample, negative ΔH_{int} values were obtained in this study, which supports the idea that the adsorbate−adsorbent interactions were mainly influenced by the hydrophobic

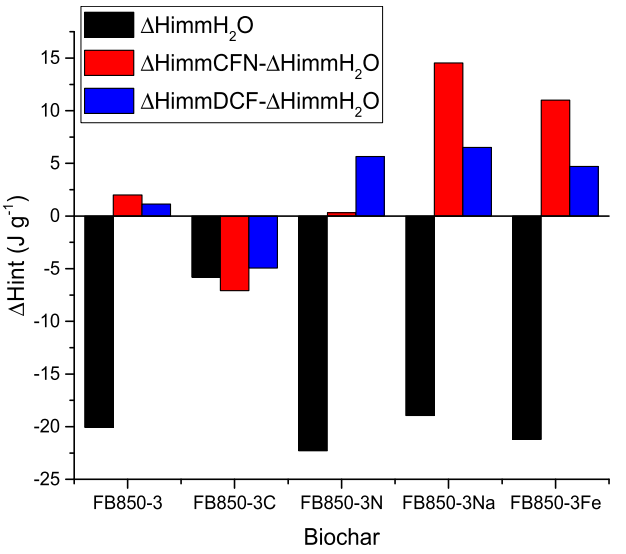

Figure 7. Enthalpy of interaction of caffeine and diclofenac at 50 mg L^{-1} and immersion enthalpy of water into fique bagasse biochar evaluated.

character of this biochar, and it is feasible to assume that the interactions happened due to factors such as (a) decreased competitive adsorption with water because in this case additional hydrogen bonds were formed and (b) the greater availability of electrons from the graphene layers in the tested FBB and the aromatic rings of CFN and DCF, which favored the formation of the $\pi-\pi$ donor−adsorbate complex.[28]

In summary, up to this point it can be stated that by using wave molecules of different molecular size it is possible to obtain the "Calorimetric PSDs" that reasonably coincide with those obtained with the classical models calculated from the isotherms of N_2 at −196.15 °C. Additionally, performing adsorbate−adsorbent studies using this technique can allow correlations with parameters such as the hydrophobic factor evaluated from immersion calorimetry in benzene and water.

3.2. Competitive Adsorption onto Fique Bagasse Biochars. In real systems, which can be solid−gas, solid−liquid, or liquid−gas, several molecules are present simultaneously; in fact, when they are considered contaminants and it is intended to eliminate them by adsorption, they compete for the active sites of the adsorbent. In order to demonstrate if the fique bagasse biochars are selective and to additionally evaluate the efficiency of these carbonaceous materials for the elimination of both caffeine and diclofenac from aquifers at different concentrations, tests were designed where these contaminants were placed in the presence of the biochars to analyze their adsorption mechanisms when the two molecules met simultaneously. The results of these competitive adsorption tests are presented in Figure 8a−f. Also (for clarity within the context of this research) in Table 2 are presented the results of two-parameter models and statistical indices on competitive adsorption of caffeine (CFN) and diclofenac (DCF) onto fique bagasse biochars evaluated at 20 °C. Additionally, Table 3 presents the results of three-parameter models and statistical indices on competitive adsorption of caffeine (CFN) and diclofenac (DCF) onto fique bagasse biochars evaluated at 20 °C.

The results presented in Tables 2 and 3 show the parameter model where the best fit is Langmuir's and its maximum adsorption capacity (Q_{max}).

https://doi.org/10.1021/acsomega.2c04872
ACS Omega 2023, 8, 1967−1978

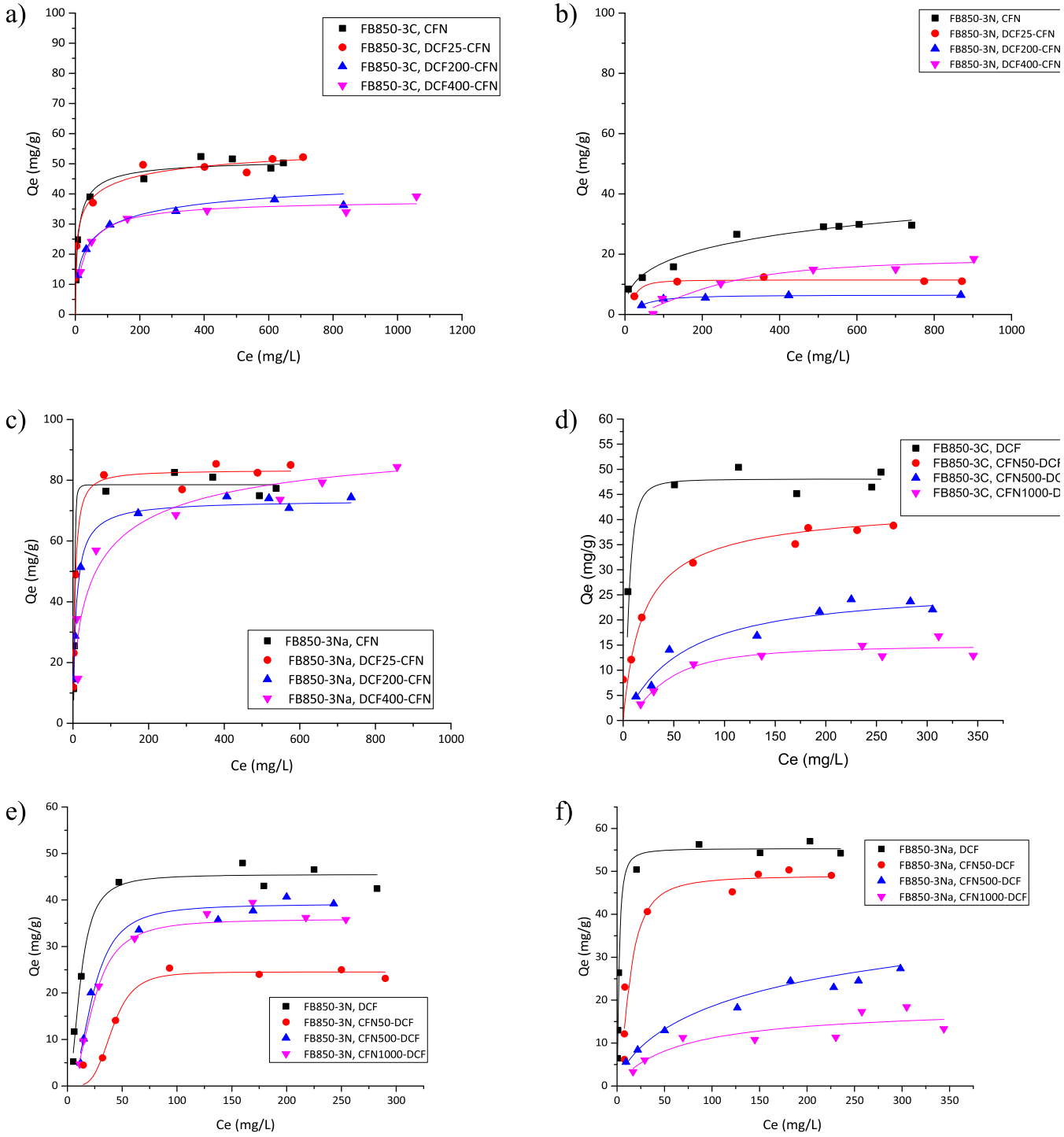

Figure 8. Competitive adsorption isotherms onto fique bagasse biochars evaluated at 20 °C: (a, b, and c) employed in each assay one different concentration of diclofenac (25, 200, and 400 mg L^{-1}) and variable caffeine quantities at range of 100−900 mg L^{-1}; (d, e, and f) used in each test one different concentration of caffeine (50, 400, and 800 mg L^{-1}) and variable diclofenac amount at range of 25−450 mg L^{-1}. (The lines correspond to the data fitted with the Sips model.)

In Table 2 it can be seen that the modified materials FB850-3C, FB850-3N, and FB850-3Na increased the adsorption capacity for both CFN and DCF with respect to the starting material, FB850-3, which is attributed to the size and distribution of the pores developed during the carbonization preparation phase and the size of the CFN and DCF molecules. That is, the diameter of the pores, which was in the range 1.36−1.82 nm, was greater than the molecular dimensions of the pollutants under study (CFN: 0.85 nm × 1.06 nm × 0.45 nm and DCF: 0.97 nm × 0.71 nm × 0.47 nm). It was facilitated by the adsorption of these compounds from the solution due to the fact that the transport within the pores was not limited by steric obstacles. Additionally, the channels of the insipient mesoporosity and macroporosity developed, together with the microporosity generated a structure that allowed the increase of the molecules under study and

https://doi.org/10.1021/acsomega.2c04872
ACS Omega 2023, 8, 1967−1978

Table 2. Results of Two-Parameter Models and Statistical Indices on Competitive Adsorption of Caffeine (CFN) and Diclofenac (DCF) onto Fique Bagasse Biochars Evaluated at 20 °C

		Langmuir[29]				Freundlich[30]			
Model/Sample		Q_{max}(mg g^{-1})	K_L (L mg^{-1})	R^2	χ^2	K_F(L g^{-1})	$1/n$	R^2	χ^2
FB850-3C	**CFN**[a]	49.4	1.71×10^{-1}	0.854	2.03	20.40	0.145	0.878	1.14
		39.3	4.13×10^{-2}	0.890	3.06	10.40	0.205	0.908	1.74
		37.3	3.70×10^{-2}	0.968	0.36	11.20	0.179	0.878	2.09
FB850-3N		17.4	1.88×10^{-2}	0.950	3.15	4.99	0.129	0.623	0.96
		6.9	2.13×10^{-2}	0.953	0.08	1.86	0.194	0.800	0.34
		28.4	1.90×10^{-3}	0.934	3.57	0.27	0.627	0.903	4.40
FB850-3Na		84.5	1.72×10^{-1}	0.990	1.13	26.40	0.194	0.864	20.50
		73.3	1.21×10^{-1}	0.941	3.26	24.10	0.178	0.818	14.90
		82.6	3.41×10^{-2}	0.891	15.70	16.40	0.248	0.889	13.10
FB850-3C	**DCF**[a]	41.8	5.07×10^{-2}	0.899	1.47	8.87	0.275	0.871	2.92
		27.6	1.63×10^{-2}	0.872	2.81	2.28	0.412	0.846	3.86
		17.3	1.89×10^{-2}	0.762	3.15	1.95	0.357	0.703	4.49
FB850-3N		31.1	1.67×10^{-2}	0.795	5.05	2.76	0.397	0.661	8.77
		49.3	2.31×10^{-2}	0.935	5.65	4.55	0.416	0.865	10.20
		42.8	2.82×10^{-2}	0.880	6.94	5.43	0.357	0.769	13.30
FB850-3Na		55.2	5.08×10^{-2}	0.913	10.70	9.04	0.330	0.836	16.60
		34.4	1.29×10^{-2}	0.877	3.81	2.21	0.451	0.876	2.93
		28.2	1.90×10^{-3}	0.790	3.56	1.67	0.391	0.772	3.46

[a]Each of the rows of the table for individual biochars relates to experiments 1, 2, and 3 of CFN and experiments 4, 5, and 6 of DCF, respectively.

Table 3. Results of Three-Parameter Models and Statistical Indices on Competitive Adsorption of Caffeine (CFN) and Diclofenac (DCF) onto Fique Bagasse Biochars Evaluated at 20°C

		Redlich–Peterson[31]					Sips[32]				
Model/Sample		K_{RP} (L g^{-1})	a_R (L mg^{-1})	B	R^2	χ^2	Q_{max} (mg g^{-1})	K_S (L g^{-1})	n_S	R^2	χ^2
FB850-3C	**CFN**[a]	18.90	0.685	0.904	0.888	0.661	61.6	0.423	0.065	0.891	0.567
		4.00	0.234	0.871	0.935	1.030	49.2	0.530	0.019	0.938	0.976
		1.61	0.054	0.967	0.972	0.315	38.2	0.885	0.035	0.970	0.336
FB850-3N		0.35	0.012	1.140	0.975	0.054	11.4	1.998	0.043	0.942	0.124
		0.12	0.011	1.070	0.963	0.060	6.4	1.530	0.022	0.973	0.037
		0.06	0.000	1.360	0.939	3.400	18.8	1.720	0.004	0.953	3.020
FB850-3Na		13.50	0.140	1.020	0.991	0.859	83.3	1.200	0.187	0.993	0.567
		8.32	0.104	1.010	0.942	3.330	73.5	0.967	0.120	0.941	3.220
		4.76	0.128	0.876	0.909	12.500	99.0	0.615	0.017	0.905	12.200
FB850-3C	**DCF**[a]	2.27	0.063	0.974	0.899	1.460	ND	ND	ND	ND	ND
		0.45	0.017	0.995	0.872	2.810	26.7	1.060	0.018	0.872	2.780
		0.26	0.005	1.190	0.769	2.900	15.0	1.580	0.026	0.776	2.750
FB850-3N		0.28	0.000	3.490	0.966	1.280	24.5	4.280	0.024	0.940	1.200
		1.33	0.003	0.872	0.949	4.450	39.1	2.280	0.043	0.969	1.910
		0.78	0.001	1.530	0.929	3.890	35.9	2.280	0.042	0.947	1.950
FB850-3Na		2.17	0.012	1.220	0.926	9.850	49.0	1.840	0.075	0.939	9.340
		0.91	0.144	0.715	0.881	2.870	49.3	0.715	0.005	0.884	2.820
		0.61	0.146	0.752	0.785	3.020	18.8	0.942	0.015	0.790	2.810

[a]Each of the rows of the table for individual biochars relates to experiments 1, 2, and 3 of CFN and experiments 4, 5, and 6 of DCF, respectively.

contributed to the greater adsorption capacity of these biochar products.

The results also show that the biochar FB850-3Na was the material that presented the highest adsorption capacity with values of 80.6 and 57.1 mg g^{-1} for CFN and DCF, respectively. While the biochars FB850-3C and FB850-3Na increased the adsorption capacity of both CFN and DCF, the FB850-3Fe decreased the CFN adsorption, all this with respect to the starting material FB850-3. This increase in the adsorption capacity in the biochar FB850-3Na is also associated with the textural characteristics of the biochar. According to the results obtained, this material is characterized by having a pore diameter (and it is possible to infer that of pore volume) appropriate for the adsorption of both CFN and DCF (V_t = 0.262 cm^3 g^{-1}), which allowed and favored the filling of the pores with the worked molecules.

On the other hand, the modified biochar FB850-3N had a percentage of smaller pores of 76%; this could benefit the adsorption of DCF and limit the retention of CFN since the DCF in its structure has 4 bonds that rotate while that CFN is completely flat, which could allow the DCF molecule to better accommodate itself to enter the pores of the FB850-3N. Meanwhile, the decrease in CFN adsorption in the biochar FB850-3Fe could happen because in this material the micropores were obstructed by the aggregates of magnetite (FexOy), with the mesopores larger than 13 nm being the

https://doi.org/10.1021/acsomega.2c04872
ACS Omega 2023, 8, 1967−1978

largest structures present in this material and from what was evidenced these pores did not favor adsorption. In addition, in relation to the series of biochar obtained at 850 °C, an increase in the adsorption capacity of both CFN and DCF was observed with the increase in the vapor residence time, and as previously mentioned, the presence of gases because of a longer time in the reactor could lead to an increase in the porosity of the carbonaceous material, which leads to better conditions for the removal of both CFN and DCF when working with unmodified fique bagasse biochar. These results are correlated with the textural characteristics previously studied by immersion calorimetry where immersion enthalpy versus PSD were correlated.

The competitive adsorption isotherms presented in Figure 8a−f show differences according to the bagasse biochar used, the adsorbate used, and the concentrations evaluated. A notable result that arises from the results obtained for the systems under study in this research is that the adsorption capacity is greater for caffeine than for diclofenac (Table 2), as was the case with the simple adsorption isotherm, where the best adsorbate in terms of adsorption capacity is presented by the sample FB850-3Na. Furthermore, the isotherms presented in Figure 7c reveal that in the sample FB850-3Na the CFN adsorption capacity varies in the range Q_e = 84.5−73.2 mg g^{-1}; meanwhile, Figure 7f shows that in FB850-3Na the capacity DCF adsorption ranges from Q_e = 55.2 to 28.2 mg g^{-1}. It is evident that the maximum adsorption capacity determined by applying the Langmuir model[29] changed less when the amount of DCF in solution was increased than when the amount of CFN in solution was increased. A similar behavior was presented when analyzing the adsorption capacity of CFN and DCF which changed for the FB850-3C sample when there was a greater quantity of these adsorbates (Q_e = 49.4−37.3 mg g^{-1} and Q_e = 41.8−17.3 mg g^{-1} for CFN and DCF, respectively).

The results found in this research are interesting and novel within the area of environmental decontamination of aquifers, especially of emerging compound waste, as is the case in this work. These show and agree with what has been proposed in this research regarding that the biochars prepared under the conditions of this work, from fique bagasse, are selective to remove caffeine in the presence of diclofenac, a system that has been simulated in the laboratory, in order to carry out an analysis closer to what is found in real systems. Furthermore, when the data from the current study were compared with the individual adsorption results (Figure 8a−f) it was evident that the adsorption capacity decreased versus the results of the competitive adsorption experiments. This complies with a competitive adsorption study of these CFN and DCF molecules on a granular activated carbon; in these tests, it was reported that a decrease in the adsorption capacity of the studied molecules usually occurs compared to individual experiments.[5]

This is associated with the characteristics of both the adsorbents (which in this case are the samples prepared from fique bagasse) and the molecules used as adsorbates (in this research CFN and DCF). As has been widely discussed during the presentation of this work, the development mainly of microporosity and the hydrophobic factor, variables that are associated with textural and chemical properties, explain that when two molecules are in the same system compared to an adsorbent, these compete with entry into the porous system. Thus, both the chemical characteristics corresponding to both CFN and DFC and the functional groups developed on the graphene layers of biochars are more related to one molecule than another so that if the pores are filled with one of molecules the other will not have enough space to enter and the adsorption differences are given in these competitive tests.

In summary, it has been widely explained that the adsorption capacity is correlated with the physicochemical properties of both biochar and the molecules under study in such a way that, considering that the caffeine molecule is smaller and flatter than the diclofenac molecule (Table 4), it can be assumed that

Table 4. Selected Properties of Caffeine and Diclofenac Sodium[34−37]

Adsorbate	Structure	Hydrogen bond donor count	Rotatable bond count	Polar surface area (Å²)	Size X Y Z (nm)
Caffeine	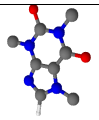	0	0	58.44	0.61 0.78 0.21
Sodium diclofenac	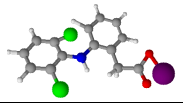	1	4	52.16	0.97 0.71 0.47

this feature facilitated the entry of CFN into the pores of the bagasse biochars more easily than DCF, thus displacing the water that could be interacting with the active sites of the FBB tested, which allows an effective contact between the CFN with the studied FBB. It is interesting to note that in an adsorption process there is competition and, in this particular case, the water molecules competed with caffeine and diclofenac for the active sites available in the biochar pores and/or it was possible that a steric hindrance of the hydrated adsorbates could occur; consequently, the interactions with the functional groups of CFN and DCF responsible for electronic interactions with the active sites of FBB were not effective.[33]

On the other hand, it has also been shown that the adsorption of compounds with different polarities on a heterogeneous surface can occur at different types of adsorbent sites, which makes competition negligible and leads to selective adsorption. The results found in this study suggest that the adsorption of DCF was due to interactions of the aromatic rings of this molecule with the graphene layers in the biochar (nonpolar interactions) while the adsorption of caffeine was due to the filling of pores and the interactions with oxygenated functional compound groups (polar interactions). Furthermore, chlorine (Cl^-) and carboxyl (COO^-) as substituent groups in the DCF molecule decrease the electron density of the molecule, which increases the adsorption efficiency in FBB through hydrophobic interactions.[33]

4. CONCLUSIONS

Values of the immersion enthalpies ($-\Delta H_{imm}$) in benzene (C_6H_6) and dichloromethane (CH_2Cl_2) changed according to the porosity of the fique bagasse biochar evaluated such that a correlation between the volume and the pore size distribution determined in the FBB and the $-\Delta H_{imm}$ calculated into benzene and dichloromethane was found. For instance, the highest $-\Delta H_{imm}$ was calculated for the FB850-3Na, which was also the carbonaceous solid with the highest proportion of

https://doi.org/10.1021/acsomega.2c04872
ACS Omega 2023, 8, 1967−1978

microporosity. On the other hand, values of $-\Delta H_{imm}$ in water did not change drastically, except for FB850-3C. These results can be justified with the data of the Boehm titrations and the infrared spectra of the FBB since these tests showed little difference on the oxygenated functional groups surface; as has been stated by other researchers, the enthalpies of immersion in water are closely related to changes in the surface chemistry and the type of organic groups present in the solids analyzed; therefore, all of the FBB prepared interacted in a similar manner with water.

For the fique bagasse biochar evaluated, the pore size distribution (PSD) was determined through density functional theory correlated with the PSD obtained by immersion calorimetry in liquids of different molecular dimensions. Furthermore, through the pore size it was evidenced that the microporosity of the FBB allowed the adsorption of CFN and DCF molecules. However, the increase of the molecule size, either by a solvation or by the formation of dimers, limited the access of these analytes to the inner porous structure of the FBB analyzed, particularly in the competitive adsorption.

It was determined that the FB850-3Na had the highest adsorption capacity in both individual and competitive tests. In addition, in the competitive experiments, the retention of CFN in this biochar was not affected significantly by the increase in the concentration of DCF; this aspect was opposed to what happened with the adsorption of DCF, which decreased as the amount of CFN increased. These results allowed us to infer that the fique bagasse biochars evaluated in competitive adsorption were selective to the removal of CFN in the presence of DCF.

■ ASSOCIATED CONTENT

Supporting Information

The Supporting Information is available free of charge at https://pubs.acs.org/doi/10.1021/acsomega.2c04872.

Brief description of calorimeter equipment used in this work, the concentrations used for competitive adsorption tests, and isotherm models used to evaluate data of competitive adsorption (PDF)

■ AUTHOR INFORMATION

Corresponding Author

Juan Carlos Moreno-Piraján − *Departamento de Química, Facultad de Ciencias, Grupo de investigación en Sólidos Porosos y Calorimetría, Universidad de los Andes, Bogotá D.C. 111711, Colombia;* orcid.org/0000-0001-9880-4696; Email: jumoreno@uniandes.edu.co

Authors

Yaned Milena Correa-Navarro − *Departamento de Química, Facultad de Ciencias Exactas y Naturales. Grupo de investigación Estudios Ambientales en Agua y Suelo, Universidad de Caldas, Manizales 170004 Caldas, Colombia; Departamento de Química, Facultad de Ciencias, Grupo de investigación en Sólidos Porosos y Calorimetría, Universidad de los Andes, Bogotá D.C. 111711, Colombia*

Liliana Giraldo − *Departamento de Química, Facultad de Ciencias, Universidad Nacional de Colombia, Sede Bogotá, Bogotá D.C. 11001, Colombia*

Complete contact information is available at: https://pubs.acs.org/10.1021/acsomega.2c04872

Notes

The authors declare no competing financial interest.

■ ACKNOWLEDGMENTS

The authors thank the Faculty of Sciences of Universidad de los Andes for partial funding through the project INV-2019-86-1819 and the Universidad de Caldas for their support for doctoral studies. The authors acknowledge the framework agreement between Universidad Nacional de Colombia and Universidad de los Andes (Bogotá, Colombia) under which this work was carried out. J.C.M.-P. also acknowledges the Facultad de Ciencias of Universidad de los Andes for the grant (No. INV-2021-128-2257).

■ REFERENCES

(1) Dabrowski, A. Adsorption—from Theory to Practice. *Adv. Colloid Interface Sci.* **2001**, *93*, 135−224.

(2) Gun'ko, V. M. Competitive Adsorption. *Theor. Exp. Chem.* **2007**, *43* (3), 139−183.

(3) Portinho, R.; Zanella, O.; Féris, L. A. Grape Stalk Application for Caffeine Removal through Adsorption. *J. Environ. Manage.* **2017**, *202*, 178−187.

(4) Acuña, V.; Ginebreda, A.; Mor, J. R.; Petrovic, M.; Sabater, S.; Sumpter, J.; Barceló, D. Balancing the Health Benefits and Environmental Risks of Pharmaceuticals: Diclofenac as an Example. *Environ. Int.* **2015**, *85*, 327−333.

(5) Sotelo, J. L.; Ovejero, G.; Rodríguez, A.; Álvarez, S.; Galán, J.; García, J. Competitive Adsorption Studies of Caffeine and Diclofenac Aqueous Solutions by Activated Carbon. *Chem. Eng. J.* **2014**, *240*, 443−453.

(6) Enders, A.; Hanley, K.; Whitman, T.; Joseph, S.; Lehmann, J. Characterization of Biochars to Evaluate Recalcitrance and Agronomic Performance. *Bioresour. Technol.* **2012**, *114*, 644−653.

(7) Igalavithana, A. D.; Mandal, S.; Niazi, N. K.; Vithanage, M.; Parikh, S. J.; Mukome, F. N. D.; Rizwan, M.; Oleszczuk, P.; Al-Wabel, M.; Bolan, N.; et al. Advances and Future Directions of Biochar Characterization Methods and Applications. *Crit. Rev. Environ. Sci. Technol.* **2018**, *3389*, 1−56.

(8) Tripathi, M.; Sahu, J. N.; Ganesan, P. Effect of Process Parameters on Production of Biochar from Biomass Waste through Pyrolysis: A Review. *Renew. Sustain. Energy Rev.* **2016**, *55*, 467−481.

(9) Akhil, D.; Lakshmi, D.; Kartik, A.; Vo, D. V. N.; Arun, J.; Gopinath, K. P. Production, Characterization, Activation and Environmental Applications of Engineered Biochar: A Review. *Environ. Chem. Lett.* **2021**, *19* (3), 2261−2297.

(10) Zhou, Y.; Qin, S.; Verma, S.; Sar, T.; Sarsaiya, S.; Ravindran, B.; Liu, T.; Sindhu, R.; Patel, A. K.; Binod, P.; et al. Production and Beneficial Impact of Biochar for Environmental Application: A Comprehensive Review. *Bioresour. Technol.* **2021**, *337* (May), 125451.

(11) Ovalle-Serrano, S. A.; Gómez, F. N.; Blanco-Tirado, C.; Combariza, M. Y. Isolation and Characterization of Cellulose Nanofibrils from Colombian Fique Decortication By-Products. *Carbohydr. Polym.* **2018**, *189* (November), 169−177.

(12) Vijayaraghavan, K. Recent Advancements in Biochar Preparation, Feedstocks, Modification, Characterization and Future Applications. *Environ. Technol. Rev.* **2019**, *8* (1), 47−64.

(13) Giraldo, L.; Rodriguez-Estupiñán, P.; Moreno-Piraján, J. C. Isosteric Heat: Comparative Study between Clausius-Clapeyron, CSK and Adsorption Calorimetry Methods. *Processes* **2019**, *7* (4), 203.

(14) Rodríguez-Reinoso, F.; Molina-Sabio, M.; González, M. T. Effect of Oxygen Surface Groups on the Immersion Enthalpy of Activated Carbons in Liquids of Different Polarity. *Langmuir* **1997**, *13* (8), 2354−2358.

(15) Correa-Navarro, Y. M.; Moreno-Piraján, J. C.; Giraldo, L. Processing of Fique Bagasse Waste into Modified Biochars for Adsorption of Caffeine and Sodium Diclofenac. *Brazilian J. Chem. Eng.* **2021**, DOI: 10.1007/s43153-021-00191-6.

(16) Silvestre-Albero, J.; Gómes de Salazar, A.; Sepúlveda-Escribano, C.; Rodriguez-Reinoso, F. Characterization of Microporous Solids by Immersion Calorimetry. *Colloids Surfaces A Physicochem. Eng. Asp.* **2001**, *187−188* (1−3), 151−165.
(17) Giraldo, L.; Huertas, J. I.; Valencia, A.; Carlos Moreno, J. A Heat Conduction Microcalorimeter for the Determination of the Immersion Heats of Activated Carbon into Phenol Aqueous Solutions. *Instrum. Sci. Technol.* **2003**, *31* (4), 385−397.
(18) Moreno, J. C.; Giraldo, L.; Gómez, A. Applicability of the Stoeckli-Bansal-Donnet Equation for the Determination of Total Area of Active Carbons by Microcalorimetry of Immersion. *Instrum. Sci. Technol.* **1998**, *26* (5), 533−541.
(19) Rouquerol, J.; Baron, G.; Denoyel, R.; Giesche, H.; Groen, J.; Klobes, P.; Levitz, P.; Neimark, A. V.; Rigby, S.; Skudas, R.; et al. Liquid Intrusion and Alternative Methods for the Characterization of Macroporous Materials (IUPAC Technical Report). *Pure Appl. Chem.* **2011**, *84* (1), 107−136.
(20) Bernal, V.; Giraldo, L.; Moreno-Piraján, J. C.; Balsamo, M.; Erto, A. Mechanisms of Methylparaben Adsorption onto Activated Carbons: Removal Tests Supported by a Calorimetric Study of the Adsorbent−Adsorbate Interactions. *Molecules* **2019**, *24* (3), 1−21.
(21) Guarín-Romero, J. R.; Rodríguez-Estupiñán, P.; Giraldo, L.; Moreno-Piraján, J. C. Simple and Competitive Adsorption Study of Nickel(II) and Chromium(III) on the Surface of the Brown Algae Durvillaea Antarctica Biomass. *ACS Omega* **2019**, *4* (19), 18147−18158.
(22) Thommes, M. Physical Adsorption Characterization of Nanoporous Materials. *Chemie Ing. Technol.* **2010**, *82* (7), 1059−1073.
(23) Acevedo, S.; Giraldo, L.; Moreno-piraja, J. C. *Enthalpies of Immersion in Benzene, Cyclohexane and Water of Granular Activated Carbons Prepared by Chemical Activation with Solutions of MgCl 2 and CaCl 2* **2015**, *121*, 1279−1285.
(24) Madani, S. H.; Hu, C.; Silvestre-Albero, A.; Biggs, M. J.; Rodríguez-Reinoso, F.; Pendleton, P. Pore Size Distributions Derived from Adsorption Isotherms, Immersion Calorimetry, and Isosteric Heats: A Comparative Study. *Carbon N. Y.* **2016**, *96*, 1106−1113.
(25) Silvestre-Albero, J.; Silvestre-Albero, A.; Rodríguez-Reinoso, F.; Thommes, M. Physical Characterization of Activated Carbons with Narrow Microporosity by Nitrogen (77.4 K), Carbon Dioxide (273 K) and Argon (87.3 K) Adsorption in Combination with Immersion Calorimetry. *Carbon N. Y.* **2012**, *50* (9), 3128−3133.
(26) Hernández-Monje, D.; Giraldo, L.; Moreno-Piraján, J. C. Data of the Immersion Enthalpy of Activated Carbon in Benzene and Cyclohexane. Influence of the Content of Surface Oxygenated Groups. *Data Br.* **2019**, *22*, 83−89.
(27) Rodríguez-Estupiñán, P.; Bastidas Barranco, M. J.; Moreno-Piraján, J. C.; Giraldo, L. A Comparison of the Energetic Interactions in the Adsorption of Co(II) from Aqueous Solution on SBA-15 and Chemically Modified Activated Carbons. *Adsorption* **2015**, *21* (8), 623−632.
(28) Bernal, V.; Erto, A.; Giraldo, L.; Moreno-Piraján, J. Effect of Solution PH on the Adsorption of Paracetamol on Chemically Modified Activated Carbons. *Molecules* **2017**, *22* (7), 1032.
(29) Langmuir, I. The Constitution and Fundamental Properties of Solids and Liquids. *J. Am. Chem. Soc.* **1916**, *38*, 2221.
(30) Freundlich, H. Adsorption in Solution. *Phys. Chem. Soc.* **1906**, *40*, 1361−1368.
(31) Redlich, O.; Peterson, D. L. A Useful Adsorption Isotherm. *J. Am. Chem. Soc.* **1959**, *63*, 1024−1025.
(32) Sips, R. Combined Form of Langmuir and Freundlich Equations. *J. Chem. Phys.* **1948**, *16*, 490−495.
(33) Álvarez, S.; Ribeiro, R. S.; Gomes, H. T.; Sotelo, J. L.; García, J. Synthesis of Carbon Xerogels and Their Application in Adsorption Studies of Caffeine and Diclofenac as Emerging Contaminants. *Chem. Eng. Res. Des.* **2015**, *95*, 229−238.
(34) Moral-Rodriguez, A. I.; Leyva-Ramos, R.; Carrasco-Marín, F.; Bautista-Toledo, M. I.; Pérez-Cadenas, A. F. Adsorption of Diclofenac from Aqueous Solution onto Carbon Xerogels: Effect of Synthesis Conditions and Presence of Bacteria. *Water. Air. Soil Pollut.* **2020**, *231* (1), 1−17.
(35) National Center for Biotechnology Information. PubChem Compound Summary for CID 5018304, Diclofenac sodium. pubchem.ncbi.nlm.nih.gov/compound/Diclofenac-sodium.
(36) National Center for Biotechnology Information. PubChem Compound Summary for CID 2519, Caffeine. https://pubchem.ncbi.nlm.nih.gov/compound/Caffeine.
(37) Pendolino, F.*Self-Assembly of Molecules on Nanostructured Graphene*; Universidad Autónoma de Madrid, 2014. DOI: 10.13140/2.1.5158.6246.

https://doi.org/10.1021/acsomega.2c04872
ACS Omega 2023, 8, 1967−1978